AFRL-ML-WP-TP-2006-441

FREEFORM EXTRUSION OF HIGH SOLIDS LOADING CERAMIC SLURRIES, PART I: EXTRUSION PROCESS MODELING (PREPRINT)

Michael S. Mason, Tieshu Huang, Robert G. Landers, Ming C. Leu, and Gregory E. Hilmas

JULY 2006

Approved for public release; distribution is unlimited.

STINFO COPY

MATERIALS AND MANUFACTURING DIRECTORATE
AIR FORCE RESEARCH LABORATORY
AIR FORCE MATERIEL COMMAND
WRIGHT-PATTERSON AIR FORCE BASE, OH 45433-7750

REPORT DOCUMENTATION PAGE

Form Approved
OMB No. 0704-0188

1. REPORT DATE *(DD-MM-YY)*	2. REPORT TYPE	3. DATES COVERED *(From - To)*
July 2006	Conference Paper Preprint	

4. TITLE AND SUBTITLE
FREEFORM EXTRUSION OF HIGH SOLIDS LOADING CERAMIC SLURRIES, PART I: EXTRUSION PROCESS MODELING (PREPRINT)

5a. CONTRACT NUMBER
FA8650-04-C-5704

5b. GRANT NUMBER

5c. PROGRAM ELEMENT NUMBER
78011F

6. AUTHOR(S)
Michael S. Mason, Robert G. Landers, and Ming C. Leu (University of Missouri-Rolla/Department of Mechanical and Aerospace Engineering)
Tieshu Huang and Gregory E. Hilmas (University of Missouri-Rolla/Department of Materials Science & Engineering)

5d. PROJECT NUMBER
2510

5e. TASK NUMBER
00

5f. WORK UNIT NUMBER
00

7. PERFORMING ORGANIZATION NAME(S) AND ADDRESS(ES)
Department of Materials Science & Engineering, and Department of Mechanical and Aerospace Engineering
1870 Miner Circle
University of Missouri-Rolla, Rolla, MO 65409–0050

8. PERFORMING ORGANIZATION REPORT NUMBER

9. SPONSORING/MONITORING AGENCY NAME(S) AND ADDRESS(ES)
Materials and Manufacturing Directorate
Air Force Research Laboratory
Air Force Materiel Command
Wright-Patterson AFB, OH 45433-7750

10. SPONSORING/MONITORING AGENCY ACRONYM(S)
AFRL-ML-WP

11. SPONSORING/MONITORING AGENCY REPORT NUMBER(S)
AFRL-ML-WP-TP-2006-441

12. DISTRIBUTION/AVAILABILITY STATEMENT
Approved for public release; distribution is unlimited.

13. SUPPLEMENTARY NOTES
This work, resulting in whole or in part from Department of the Air Force contract FA8650-04-C-5704, has been submitted for publication in the 2006 Freeform Fabrication Symposium Proceedings. If this work is published, the publisher may assert copyright. The United States has for itself and others acting on its behalf an unlimited, paid-up, nonexclusive, irrevocable worldwide license to use, modify, reproduce, release, perform, display, or disclose the work by or on behalf of the Government. All other rights are reserved by the copyright owner. PAO Case Number: AFRL/WS 06-1754, 13 Jul 2006. Paper contains color.

14. ABSTRACT
A novel, solid freeform fabrication method has been developed for the manufacture of ceramic-based components in an environmentally friendly fashion. The method is based on the extrusion of ceramic slurries using water as the binding media. Aluminum oxide (Al_2O_3) is currently being used as the part material and solids loading as high as 60 vol. % has been achieved. This paper describes a novel manufacturing machine that has been developed for the extrusion of high solids loading ceramic slurries. A critical component of the machine is the deposition system, which consists of a syringe, a plunger, a ram actuated by a motor that forces the plunger down to extrude material, and a load cell to measure the extrusion force. An empirical, dynamic model of the ceramic extrusion process, where the input is the commanded ram velocity and the output is the extrusion force, is developed. Several experiments are conducted and curve fitting techniques are utilized to construct the dynamic model. The results demonstrate that the ceramic extrusion process has a very slow dynamic response, as compared to other non-compressible fluids such as water. A substantial amount of variation exists in the ceramic extrusion process, most notably in the transient dynamics, and a constant ram velocity may either produce a relatively constant steady-state extrusion force or it may cause the extrusion force to steadily increase until the ram motor skips. The ceramic extrusion process is also subjected to significant disturbances such as air bubble release, which causes a dramatic decrease in the extrusion force, and nozzle clogging, which causes the extrusion force to slowly increase until the clog is released or the ram motor skips.

15. SUBJECT TERMS Ceramic, slurry, extrusion, freeform

16. SECURITY CLASSIFICATION OF:			17. LIMITATION OF ABSTRACT:	18. NUMBER OF PAGES	19a. NAME OF RESPONSIBLE PERSON (Monitor)
a. REPORT	b. ABSTRACT	c. THIS PAGE			Mary E. Kinsella
Unclassified	Unclassified	Unclassified	SAR	20	19b. TELEPHONE NUMBER *(Include Area Code)* N/A

Freeform Extrusion of High Solids Loading Ceramic Slurries, Part I: Extrusion Process Modeling

Michael S. Mason[1], Tieshu Huang[2], Robert G. Landers[1],
Ming C. Leu[1], and Gregory E. Hilmas[2]

1870 Miner Circle
Department of Mechanical and Aerospace Engineering[1]
Department of Materials Science and Engineering[2]
University of Missouri at Rolla, Rolla, Missouri 65409–0050
{mmason,hts,landersr,mleu,ghilmas}@umr.edu

ABSTRACT

A novel, solid freeform fabrication method has been developed for the manufacture of ceramic-based components in an environmentally friendly fashion. The method is based on the extrusion of ceramic slurries using water as the binding media. Aluminum oxide (Al_2O_3) is currently being used as the part material and solids loading as high as 60 vol. % has been achieved. This paper describes a novel manufacturing machine that has been developed for the extrusion of high solids loading ceramic slurries. A critical component of the machine is the deposition system, which consists of a syringe, a plunger, a ram actuated by a motor that forces the plunger down to extrude material, and a load cell to measure the extrusion force. An empirical, dynamic model of the ceramic extrusion process, where the input is the commanded ram velocity and the output is the extrusion force, is developed. Several experiments are conducted and curve fitting techniques are utilized to construct the dynamic model. The results demonstrate that the ceramic extrusion process has a very slow dynamic response, as compared to other non-compressible fluids such as water. A substantial amount of variation exists in the ceramic extrusion process, most notably in the transient dynamics, and a constant ram velocity may either produce a relatively constant steady-state extrusion force or it may cause the extrusion force to steadily increase until the ram motor skips. The ceramic extrusion process is also subjected to significant disturbances such as air bubble release, which causes a dramatic decrease in the extrusion force, and nozzle clogging, which causes the extrusion force to slowly increase until the clog is released or the ram motor skips.

1. INTRODUCTION

There have been only a handful of novel SFF systems described in the literature over the past several years [1-7]. Most of these systems have utilized 3D gantry positioning systems. Malone [2] explains that 3D gantries have easy maneuverability and high payload capacities. The emphasis in this work was on high motor accelerations so that a constant deposition feed rate could be utilized. Weiss and Prinz [4] have also developed this type of system for customized solid freeform fabrication processes. Some improvements have also been made to the Selective Laser Sintering (SLS) process by reducing the amount of material being heated, thereby improving part accuracy [5-6]. Other areas of improvement have been in Stereolithography by reducing the part shrinkage that is inherent within the process [7]. Freeze-

form Extrusion Fabrication (FEF) is a new SFF process that deposits ceramic slurry utilizing extrusion in a layer by layer fashion to create 3D geometries [8]. The FEF system uses a different approach in mechanical implementation as compared to most other SFF processes. Similar to Rapid Freeze Prototyping (RFP) [9-12] an XY table with a third separate Z elevator axis is used. The 3D gantry and the XY table with Z elevator operate on the same principle. The 3D gantry has all three axes connected into a single unit, which forces the axes to be level with respect to each other, within a specified tolerance, before installation. The XY table and Z elevator are individually known to be level, but the axes must be adjusted to be level relative to each other during installation.

A large amount of ceramic flow modeling has been done previously. Benbow and Bridgewater have developed the standard model for this process [13]. The only problem with this model is that it is a static relationship between ram velocity and applied force. Other modifications of this model have been developed [14] but always keeping a static model. It is the authors' goal to develop a dynamic model in order to optimize the extrusion process.

In the following sections the FEF system will be described in detail, highlighting the major process parameters. The ceramic high solids loading slurry extrusion process will be examined, including system disturbances. In the second section each piece of hardware comprising the FEF system is described, as well as its function and its interaction with other hardware components. In the third section the extrusion process is described. First, the internal system disturbances are described along with the effects they have on the extrusion process. Then experimental tests are conducted to characterize the behavior of the extrusion process.

2. EXPERIMENTAL SETUP

The FEF experimental setup is composed of three major components: the motion system, the real-time data acquisition and control system, and the extrusion device. Each of the components can be decomposed into several sub components, which are described below. A picture of the complete system is shown in Figure 1.

Three Empire Magnetic extended temperature range stepper motors are used to drive Parker Hannifin Daedal 404 XR series linear axes. The three orthogonal linear axes each have 254 *mm* of travel, forming a three-dimensional motion system. The stepper motors have a stepping angle of 1.8 degrees, but have the ability to utilize "micro steps." Micro steps give a motor the ability to take multiple smaller steps to reach a single stepping angle. The stepper motors can vary the micro steps from 1-250 *microsteps/full step* giving a maximum possible resolution of 0.0072 *degrees/step*. The resolution of each axis is 2.5 μm per step, or 0.1 μm per micro-step, when using 250 *microsteps/full step*. The motors have a maximum velocity of 50 *rev/s*, which provides a maximum velocity of 250 *mm/s* for the individual axes. The maximum motor acceleration is 50 rev/s^2, which provides a maximum linear axis acceleration of 250 mm/s^2.

An extrusion device capable of exerting high pressures is necessary for deposition of high solids loaded ceramics. A stepper motor with a resolution of 16,000 *steps/inch* and maximum velocity of 15 *inches/s* is directly coupled to the Z-axis. The extrusion axis, having eight inches of stroke is used to move a plunging device, which applies pressure to a syringe to extrude ceramic material. The deposition rate can be changed online by adjusting the commanded stepper motor speed. A 60 cm^3 syringe is used to hold and eject the deposition material. Nozzles

of varying diameters ranging from 190 – 580 μm are attached to the end of the syringe to allow for different thicknesses of material to be deposited.

A LC-305 load cell from Omega Engineering is utilized for force feedback. The load cell measures the extrusion force of the ram extruder on the ceramic slurry. The load cell outputs a differential voltage (0 – 20 mV) that corresponds to the extruded force (0 – 4450 N). This signal is sent to an amplifier that increases the differential voltage by a factor of 100, thus, the output range is 0 – 2 V. This increases the input range thereby increasing the overall resolution of the feedback device. The load cell has a 0.1% linearity, which gives an output within +/- 4.45 N of the actual force.

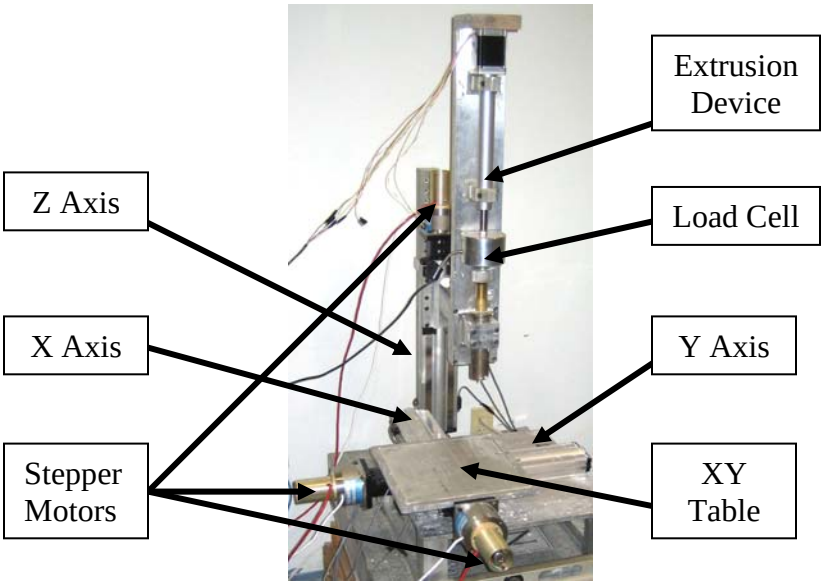

Figure 1: Picture of FEF experimental setup.

3. FLOWRATE MODELING

In modeling and controlling the ceramic slurry extrusion process, one must consider the system disturbances and material flowrate dynamics. The first subsection describes in detail the two major disturbances that are present within the system: agglomerate breakdown and air bubble release. The next section explains the different types of material flowrate tests conducted in order to characterize the dynamic extrusion process.

3.1 System Disturbances

There are two major disturbances that occur during the extrusion process: agglomerate breakdown and air bubble release. Both of these disturbances cause changes to the ceramic slurry flowrate. The following sections explain why the disturbances are present and how they affect the extrusion process.

3.1.1 Agglomerate Breakdown Ceramic slurries are fluids with significant solids loading. In the case of the FEF process, the solids loading is higher, generally greater than 50 vol. %. The solid particles that are present within the slurry are referred to as agglomerates. When batching

the ceramic slurry the ceramic powder is mixed with an aqueous media. The current ceramic of interest is alumina Al_2O_3, in combination with water as the binding media, Polyethelene-Glycol for improved green part strength, and Aquazol for material lubrication. The materials are mixed for a period of time to form an isotropic slurry. The ceramic particle size is reduced as much as possible, generally ranging from 0.8 to 2.5 μm. With particles of varying size it becomes increasingly difficult for the particles to be evenly interspersed within the aqueous media. The ceramic particles join together into larger particles called agglomerates. The agglomerates are interspersed within the aqueous media, thereby forming the ceramic slurry.

For the FEF system an extrusion process is utilized. As force is applied to the ceramic slurry, the material reservoir compresses due to the presence of air bubbles (described later), and material flowrate increases with the rising force. After compression is complete the material flowrate reaches a stable state. As the material enters the nozzle, the space available for agglomerates to be interspersed is significantly reduced. This causes an increase in resistance force for compression of the slurry since the agglomerates are pressed together. After a critical force is reached the agglomerates "slide" across edges of other agglomerates. During the sliding process the agglomerates break into smaller agglomerates allowing for material flow to continue. Figure 2 shows an example of agglomerate breakdown.

The force spikes caused by agglomerate breakdown cannot be reliably predicted. The agglomerate size is random and is different for each slurry preparation. The breakdown of the agglomerates also occurs randomly, but can be reduced by minimizing the ceramic particle size.

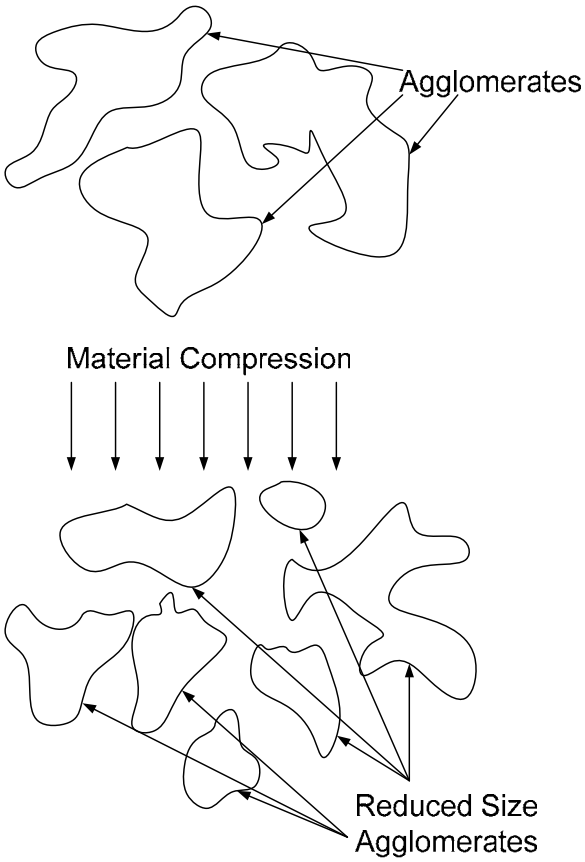

Figure 2: Example of agglomerate breakdown.

3.1.2 Entrapped Air Bubble Release During the preparation phase of the ceramic slurry, the slurry is mixed in a vacuum to remove air present within the slurry for a more consistent fluid. After the slurry is mixed, it must be loaded into the fluid reservoir. Due to the high solids loading the fluid is extremely viscous requiring manual loading of the material. During the loading process air becomes entrapped within the ceramic slurry. After the reservoir is full, it is then sealed for future use during an extrusion process. As the ram applies force to the ceramic slurry, the air bubbles compress due to buoyancy effects from the surrounding slurry. As material is extruded the air bubbles are forced into the die region, which is a much smaller region than the rest of the syringe. The air bubbles join together as they enter the die region, forming larger bubbles (Figure 4). As the bubbles reach the nozzle exit they pop and create a large pressure release. The region previously occupied by the bubble is now empty allowing for the ceramic slurry to expand.

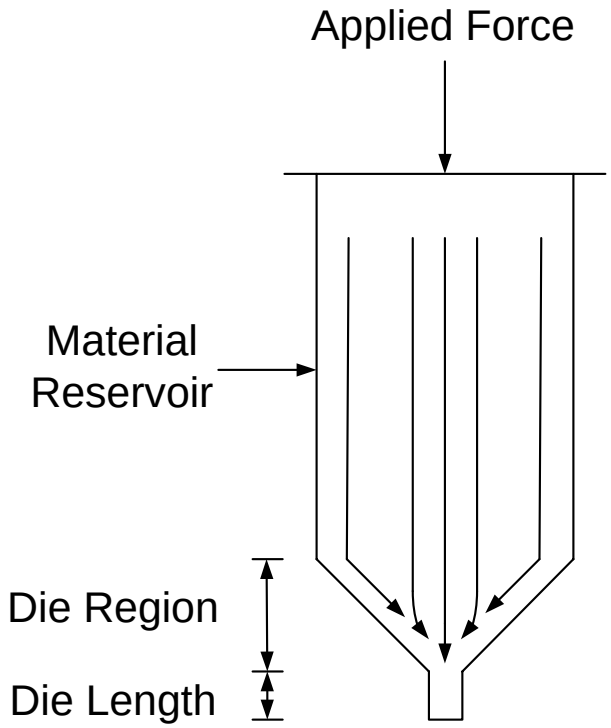

Figure 3: Example of slurry flow within material reservoir.

3.2 Flowrate Tests

For modeling the ram extrusion process two different types of tests were conducted. It was first necessary to determine a ram velocity operational range. This was determined by running the ram extrusion velocity at various speeds and visually inspecting the extrudate for curling and clogging. Curling is the phenomenon where the extrudate curls on the nozzle tip, as shown in Figure 5. Clogging is when extrudate dries within the nozzle and reduces the material flowrate until no material can be extruded through the nozzle. Neither of these situations are desirable for extrusion. The upper and lower ram velocity limits were determined empirically and the extrusion speed ROI for the ceramic slurries considered in this paper is 0.2 to 0.65 $\mu m/s$. Velocities below the lower range lead to clogging, while velocities above the higher range cause

curling, which will eventually lead to clogging. It should be noted that velocities outside the operational range can be used, but only for short periods of time.

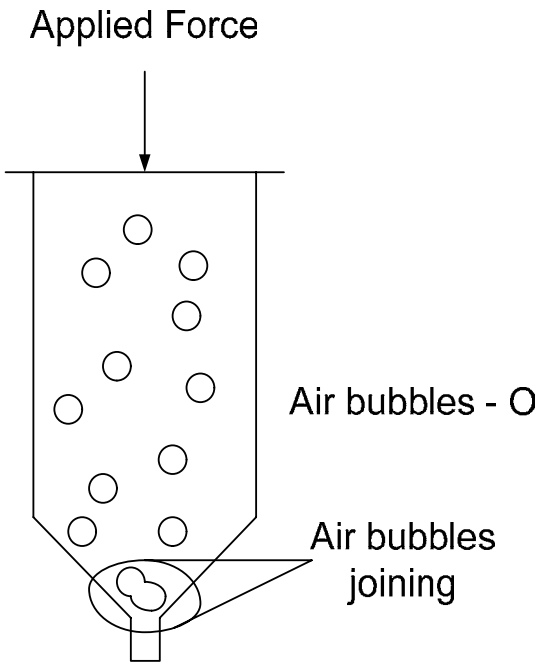

Figure 4: Example of entrapped air bubbles within material reservoir.

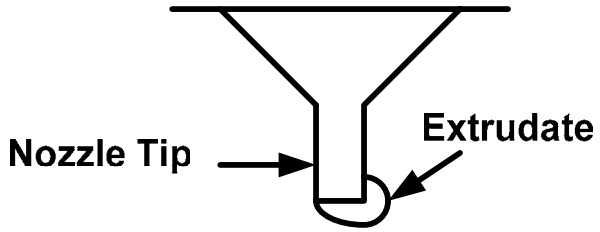

Figure 5: Curling of extrudate on nozzle tip.

3.2.1 Long Step Tests A series of step tests with constant ram velocities were conducted first. The commanded ram velocity was kept constant for one hour and extrusion force and mass data were collected at a rate of 1 *Hz*. The mass data was collected through a mass balance connected to the PC through a USB port. The mass balance was set to a baud rate of 9200 and continuous acquisition. A total of seven tests were conducted at different velocities within the range of interest using a 190 μm diameter nozzle. The collected extrusion force data illustrates the dynamic behavior that is created by applying constant ram velocities. During most of the tests a somewhat steady state force was reached, implying that extrusion force and ram velocity are related. Curve fitting was performed to determine a model for each test conducted. A first order model of the form

$$\frac{F(s)}{v(s)} = \frac{K}{\tau s + 1} \tag{1}$$

where K is the gain and τ is the time constant were fit to each set of experimental data. To find the steady-state force an average was taken over the region following the initial force rise. The

time constant varied for each of the extrusion velocities, but each was found to be at a minimum 200 *s*. Table 1 shows the ram velocity, time constant, gain, and steady state extrusion force for each test. Figures 6-8 show some of the step test data. Figures 7 and 8 show that the process is not repeatable, for the same inputs test 2 reaches a steady-state force value of 180 *N*, but test 3 continues to increase during the entire testing period. Test 3 had an initial extrusion force value of approximately 50 *N*, which is a different starting condition than test 2, but this should cause the extrusion force to reach the steady state value quicker.

Table 1: Data for constant velocity step tests.

Test (#)	v (μm/s)	τ (sec)	K (N/μm/s)	F_{ss} (N)	m (mg/s)
1	0.3	200	433	130	29.9
2	0.4	200	450	180	36.1
3	0.4	----------	----------	----------	----------
4	0.45	500	467	210	36.8
5	0.45	600	644	290	46.1
6	0.5	250	500	250	45.0
7	0.55	900	564	310	50.0
8	0.6	225	533	320	55.0
9	0.6	----------	----------	----------	----------
	Average	319	513		
	σ	268	74		

Tests 3 and 9 did not reach steady state during the one hour time period and were therefore not included in the linear relationships found. The large time constant demonstrated that the ceramic slurry extrusion process is extremely slow as compared to other incompressible fluid flow systems such as water where the time constant is on the order of 10 *ms* [15]. The larger time constant value is partially due to the viscosity of the ceramic slurry. If the slurry is a non-Newtonian fluid, then the viscosity increases with increasing fluid shear rate, which is directly affected by the ram velocity. Future work will need to be conducted to investigate this hypothesis.

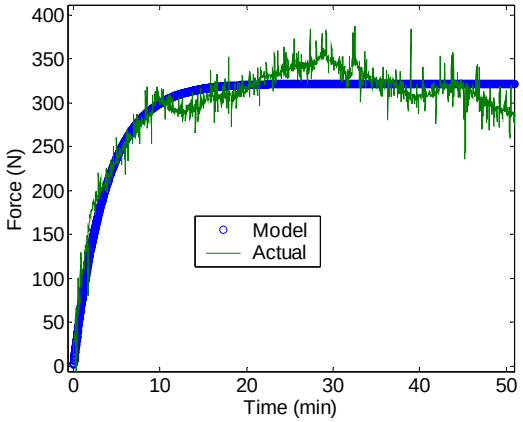

Figure 6: Constant velocity flowrate test (8) with ram extrusion v = 0.6 $\mu m/s$ and F_{ss} = 320 N.

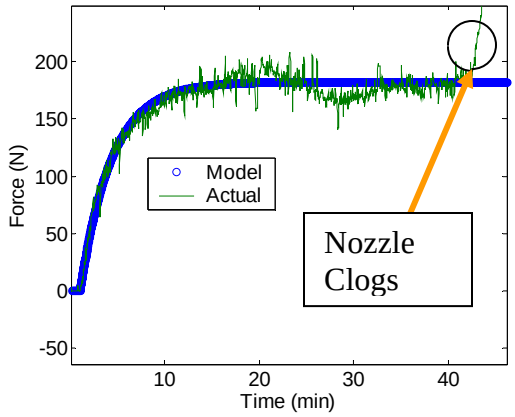

Figure 7: Constant velocity flowrate test (2) with ram extrusion v = 0.4 $\mu m/s$ and F_{ss} = 180 N.

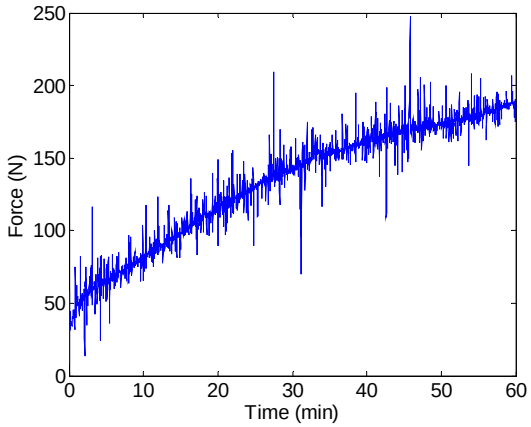

Figure 8: Constant velocity flowrate test (3) with ram extrusion v = 0.4 $\mu m/s$.

A linear least squares curve fit was utilized to relate the three parameters, steady state extrusion force, ram velocity, and mass flowrate, to each other. Three relationships were considered: mass flowrate versus extrusion force, mass flowrate versus ram velocity, and extrusion force versus ram velocity. Equations 2-4 show the relationships between the three parameters (mass flowrate, extrusion force, and ram velocity) and Figures 9 to 11 show the test data with the linear relationships. Even though the y intercept values were determined there is no physical meaning to them because equations (2) – (4) are only valid for ram velocities in the range of 0.3-0.6 μms/s. There are short term dynamics present that are not considered in these relationships.

$$\frac{\Delta m_{ss}}{\Delta F_{ss}} = 0.70 \tag{2}$$

$$\frac{\Delta m_{ss}}{\Delta v_{ss}} = 50 \tag{3}$$

$$\frac{\Delta F_{ss}}{\Delta v_{ss}} = 140 \tag{4}$$

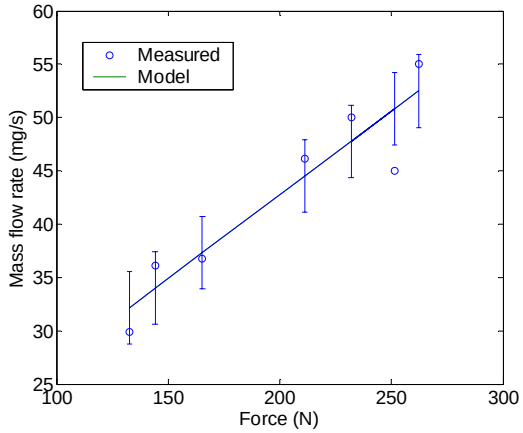

Figure 9: Steady-state mass flowrate versus steady-state extrusion force. Error bar corresponds to one standard deviation.

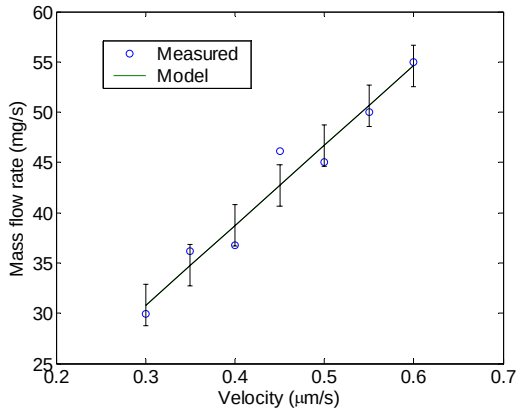

Figure 10: Steady-state mass flowrate versus steady-state ram velocity. Error bar corresponds to one standard deviation.

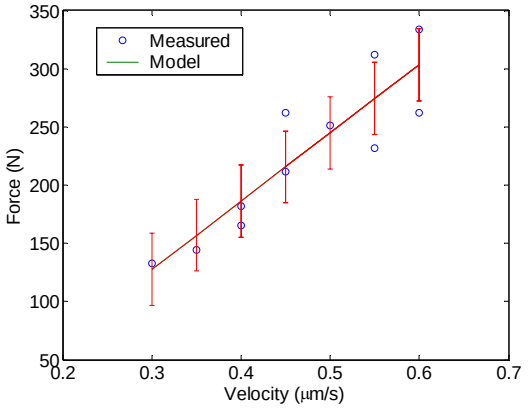

Figure 11: Steady-state extrusion force versus steady-state ram velocity. Error bar corresponds to one standard deviation.

One standard deviation of the curve fit is shown by the error bars. The standard deviations are 3.4 *mg/s*, 2.1 *mg/s*, and 29 *N* for equations (2)-(4), respectively. As can be seen

from the figures, there is a definite correlation relating the three parameters. The correlation coefficients for mass flowrate to extrusion force, mass flowrate to ram velocity, and extrusion force to velocity are 0.9356, 0.9764, and 0.9123, respectively.

3.2.2 Short Step Test The next test conducted was a short step test in which the ram extruder ran at velocities covering the ROI. The velocities varied by +/-0.05 *μm/s* with 40 *sec* time periods. The initial velocity was run for a period of 8 *min*, which was determined to be the average time for a given ram velocity to reach a steady-state extrusion force, in order for the extrusion force to reach steady-state before the test was started. The time history of the commanded velocity and corresponding extrusion force are shown in Figure 12. Force data was collected at a rate of 20 *Hz*.

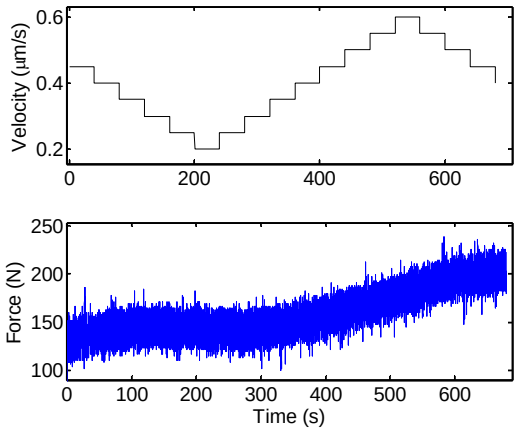

Figure 12: Ram velocity and extrusion force time history for the short step test.

It would be assumed that the extrusion force would increase with an increase in ram velocity. After examining the extrusion force data it can be seen there is a delayed reaction between the change in ram velocity and the change in the extrusion force. The ram velocity decreases by 0.05 *μm/sec* for the first 5 time periods, but the extrusion force does not start to decrease until 200 *sec* at which point the ram velocity has dropped 0.25 μm/s down to 0.2 *μm/sec*. At 240 *sec* the ram velocity is increased to 0.25 *μm/sec*, but the extrusion force continues to decrease until 280 *sec*. At this time the ram velocity is 0.3 *μm/sec*. The ram velocity continues to increase up to 0.6 *μm/sec* at 520 *sec* while the extrusion force keeps increasing until 640 *sec* two time periods after the ram velocity has been decreased. During the remaining time the extrusion force levels out. Another interesting trend that can be seen in Figure 12 is that the extrusion force increases at a faster rate with increasing velocity than the force decreases with decreasing velocity, which is believed to be due to material compression effects.

3.2.3 Impact Tests The third type of flowrate tests conducted were impact tests. These tests consisted of applying a constant ram velocity for a fixed period of time and then reducing the ram velocity for the same period of time. This ram velocity cycle is repeated for the entire test. The extrusion force is collected to examine the effects of the ram velocity. This test shows the effect that the current extrusion force has on the increase/decrease of the force due to the change in ram velocity.

Two different types of impact tests were conducted to determine the influence of a higher ram velocity on the extrusion force. Force data was collected at a rate of 10 *Hz*. The first test conducted had lower ram velocities of 0.5 *μm/s* and higher ram velocities that increased by 5 *μm/s* every other time period. Figure 13 shows the results. As can be seen the higher the ram velocity the faster the increase in extrusion force. There is a delayed reaction between the change in ram velocity and change in extrusion force. The delay is 0-9 *sec*. Application of the chosen ram velocities rapidly increased the extrusion force to the motor limit so only one test was conducted.

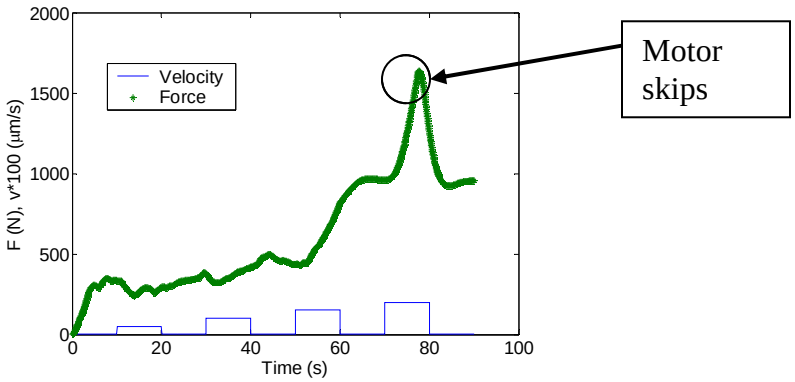

Figure 13: Impact test with increasing velocity inputs.

The second flowrate impact test conducted repeatedly changed the ram velocity between 0.5 and 5 *μm/s* every 40 *sec*. The extrusion force increased and decreased at a faster rate with a higher current extrusion force value. The application periods were too long thereby causing the motor to skip as shown in Figure 14. The time period was then reduced to 10 *sec* for the last two test runs. Figure 15 shows more clearly the effect the value of the current force has on the increasing/decreasing effect. The 0-9 *sec* delay is present for every change in velocity input. With a total of 73 individual ram velocity changes it was visually examined that the delay for increasing ram velocity was higher than for decreasing ram velocity. The average delay for increasing ram velocity was 4.3 *sec* with a standard deviation of 1.31 *sec* as calculated from 37 ram velocity increases. The average delay for decreasing ram velocity was 2.5 *sec* with a standard deviation of 1.5 *sec* calculated from 36 ram velocity decreases. The delay is not present in the long step tests though. This would indicate that an extrusion force causes a delay with a change in ram velocity. The delay in the force reaction supports the data collected from the previous two tests in that the system is slow to react to the input.

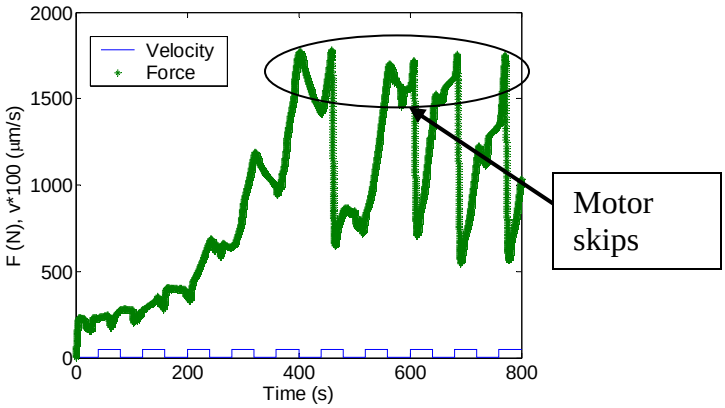

Figure 14: Constant level velocity input for 40 *s* periods.

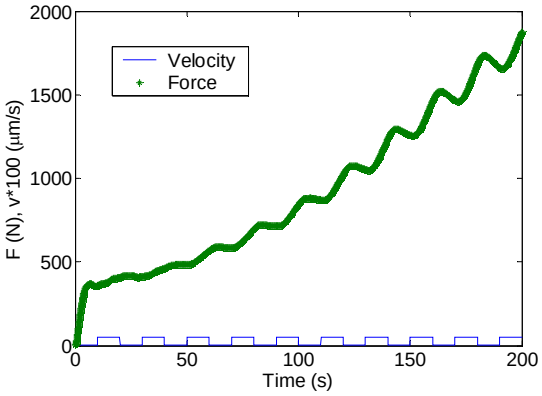

Figure 15: Repeated velocity input for 10 *s* periods.

4. SUMMARY AND CONCLUSIONS

A new environmentally friendly solid freeform fabrication technique, Freeze-form Extrusion Fabrication (FEF), has been developed utilizing aqueous ceramic slurries as the build material. The FEF system was described in detail highlighting the major hardware components. System disturbances were described along with their effects on flowrate behavior. Multiple tests were conducted in order to characterize the ceramic slurry flow utilizing a ram extruder. A first order process model was developed and compared to collected data.

From the extrusion tests conducted it was shown that the fluid flowrate is much slower when compared to other incompressible fluid flows such as water from the large time constant values. There is a large variability in the value of the time constant, leading to the fact that the process is non repeatable. From the impact tests it was shown that different dynamics are present between increasing and decreasing extrusion force due to a faster increase in extrusion force from higher ram velocities than a decrease in extrusion force due to a reduction in ram velocity.

ACKNOWLEDGEMENTS

This work was supported by the Air Force Research Laboratory under Contract FA8650-04-C-5704. The authors would also like to thank Mike Hayes of Boeing for his technical support and Justin Kayser for time and effort in this research.

REFERENCES

1. K. Taminger, R. Hafley, D. Fahringer, and E. Martin, "Effect of Surface Treatments on Electron Beam Freeform Fabricated Aluminum Structures," Langley Technical Reports (2004).
2. E. Malone, R. Rasa, D. Cohen, T. Isaacson, H. Lashley, and H. Lipson, "Freeform Fabrication of 3D Zinc-Air Batteries and Functional Electro-Mechanical Assemblies," *Rapid Prototyping Journal*, Vol. 10, No. 1, 58-69 (2004).
3. H. Lipson and J.B. Pollack, "Automatic Design and Manufacture of Artificial Lifeforms," *Nature*, Vol. 406, 974-978 (2000).
4. L. Weiss and F. Prinz, "Novel Applications and Implementations of Shape Deposition Manufacturing," Naval Research Reviews, Vol. 1, Office of Naval Research, (1998).
5. H. Gothait, Object Geometries, Patent 6850334 (2000).
6. B. Jang, J. Duan, K. Chen, and E. Ma, Nanotek Instruments Inc., Patent 6405095 (2002).
7. M. Guertin, C. Hull, and H. Nguyen, 3D Systems, Patent 6399010 (2002).
8. T. Huang, M. Mason, G. Hilmas, and M. C. Leu, "Freeze-form Extrusion Fabrication of Ceramics," *Proceedings of Solid Freeform Fabrication Symposium*, August 1-3, Austin, Texas, 72-85 (2005).
9. G. Sui, "Modeling and Analysis of Rapid Freeze Prototyping," PhD Dissertation, University of Missouri-Rolla, Rolla, Missouri (2002).
10. F. Bryant, G. Sui, and M. C. Leu, "A Study on the Effects of Process Parameters in Rapid Freeze Prototyping," *Proceedings of Solid Freeform Fabrication Symposium*, August 5-7, Austin, Texas, 635-642 (2002).
11. M. C. Leu, W. Zhang, and G. Sui, "An Experimental and Analytical Study of Ice Part Fabrication with Rapid Freeze Prototyping," *Annals of the CIRP*, Vol. 49/1, 147-150 (2000).
12. G. Sui, and M. C. Leu, "Investigation of Layer Thickness and Surface Roughness in Rapid Freeze Prototyping," *ASME Journal of Manufacturing Science Engineering*, Vol. 125/3, 555-563 (2002).
13. J. Benbow and J. Bridgwater, *Paste Flow and Extrusion, Oxford Series on Advanced Manufacturing*, Vol. 10, Clarendon Press, Oxford, (1993).
14. P. Martin, D. Wilson, and K. Challis, "Extrusion of Paste Through Non-Axisymetric Systems" *6th World Congress of Chemical Engineering*, Melbourne, Australia, September 23-27 (2001).

15. M. Munson, D. Young, and T. Okiishi, Fundamentals of Fluid Mechanics, Thierd Edition, New York, John Wiley and Sons Inc., 462-468 (1998).